AD-A277 296

NAVAL POSTGRADUATE SCHOOL
Monterey, California

DTIC
ELECTE
MAR 28 1994
S E D

THESIS

A NONLINERAR STUDY OF THE GAIN MARGIN
OF A THIRD ORDER   REGULATOR SYSTEM

by

Dimopoulos Ilias

December 93

Thesis Advisor: PAPOULIAS FOTIS

94-09395

Approved for public release; distribution is
unlimited.

94 3 25 097

REPORT DOCUMENTATION PAGE

Form Approved
OMB No. 0704-0188

1. AGENCY USE ONLY *(Leave blank)*	2. REPORT DATE December 1993	3. REPORT TYPE AND DATES COVERED Master's Thesis

4. TITLE AND SUBTITLE

A Non-linear Study of the Gain Margin of a Third Order Regulator System

5. FUNDING NUMBERS

6. AUTHOR(S)

LCOL Ilias Dimopoulos

7. PERFORMING ORGANIZATION NAME(S) AND ADDRESS(ES)

Naval Post Graduate School
Monterey, CA 93943

8. PERFORMING ORGANIZATION REPORT NUMBER

9. SPONSORING/MONITORING AGENCY NAME(S) AND ADDRESS(ES)

10. SPONSORING/MONITORING AGENCY REPORT NUMBER

11. SUPPLEMENTARY NOTES

The views expressed in this thesis are those of the author and do not reflect the official policy or position of the Department of Defense or the U.S. Government.

12a. DISTRIBUTION/AVAILABILITY STATEMENT

Approved for public release; distribution is unlimited.

12b. DISTRIBUTION CODE

A

13. ABSTRACT *(Maximum 200 words)*

This thesis analyzes the dynamic response of a third order regulator system. Particular emphasis is placed upon the loss of stability of the nominal equilibrium state. The system utilized in this research models the fundamental turning dynamics of an autonomous vehicle. We make extensive use of bifurcation theory methods in analyzing the dynamics after initial loss of stability. The effective gain of the system is used as the main bifurcation parameter, since this is directly related to the gain margin for linear systems. It is shown that the nonlinear characteristics of the system may significantly affect the practical significance of its gain margin, as a measure of robustness to parameter variations, unmodeled dynamics, and external disturbances.

14. SUBJECT TERMS

Control, Gain Margin, Stability, Bifurcation

15. NUMBER OF PAGES

39

16. PRICE CODE

17. SECURITY CLASSIFICATION OF REPORT	18. SECURITY CLASSIFICATION OF THIS PAGE	19. SECURITY CLASSIFICATION OF ABSTRACT	20. LIMITATION OF ABSTRACT
Unclassified	Unclassified	Unclassified	UL

NSN 7540-01-280-5500

Standard Form 298 (Rev 2-89)
Prescribed by ANSI Std Z39-18
298-102

A Nonlinear Study of the Gain Margin of a Third Order Regulator System

by

Ilias Dimopoulos
Lieutenant Colonel, Hellenic Army
B.S., Hellenic Army Academy, 1976
Diploma, National Technical University of Athens, 1983

Submitted in partial fulfillment of the
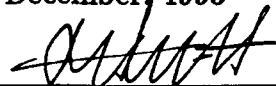requirements for the degree of

MASTER OF SCIENCE IN ELECTRICAL ENGINEERING

from the

NAVAL POSTGRADUATE SCHOOL
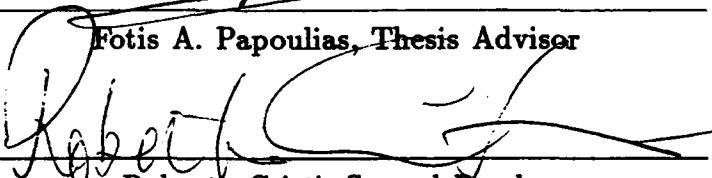
December, 1993

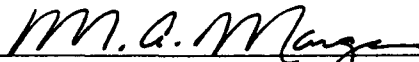Author: _____ Dimopoulos I.
Ilias Dimopoulos

Approved by: _____
Fotis A. Papoulias, Thesis Advisor

_____
Roberto Cristi, Second Reader

_____
Michael A. Morgan, Chairman
Department of Electrical and Computer Engineering

ii

ABSTRACT

This thesis analyzes the dynamic response of a third order regulator system. Particular emphasis is placed upon the loss of stability of the nominal equilibrium state. The system utilized in this research models the fundamental turning dynamics of an autonomous vehicle. We make extensive use of bifurcation theory methods in analyzing the dynamics after initial loss of stability. The effective gain of the system is used as the main bifurcation parameter, since this is directly related to the gain margin for linear systems. It is shown that the nonlinear characteristics of the system may significantly affect the practical significance of its gain margin, as a measure of robustness to parameter variations, unmodeled dynamics, and external disturbances.

Accesion For		
NTIS CRA&I		☒
DTIC TAB		☐
Unannounced		☐
Justification		
By		
Distribution /		
Availability Codes		
Dist	Avail and / or Special	
A-1		

TABLE OF CONTENTS

I. INTRODUCTION

A. PROBLEM STATEMENT

It is well known that in linear dynamical systems one of the most popular ways of assessing the stability properties of the system is through its gain margin (Friedland, 1986). Roughly speaking, the gain margin designates the extent at which the effective gain of the system can be increased before loss of stability occurs. Therefore, it is widely used in linear control system design in order to quantify a measure of robustness of the system with regards to parameter variations, disturbances, and unmodelled dynamics.

In this work we examine the concept of gain margin in the light of nonlinear systems. We assume that the baseline linear system is an approximation to a nonlinear system. For demonstration purposes we employ a third order, single input single output system, with cubic nonlinearities. This system models the fundamental turning dynamics of a marine vehicle (Oral, 1993). Primary loss of stability is shown to occur in the form of generic bifurcations to periodic solutions (Guckenheimer & Holmes, 1983). We use center manifold reduction techniques and integral averaging in order to capture the stability properties of the resulting limit cycles (Chow & Mallet–Paret, 1977). The main conclusion of this work is that the linear concept of a gain margin can be used as a reliable measure of stability only in the case of supercritical bifurcations to periodic solutions. In the case of subcritical bifurcations, a

1

modification is necessary which is based on the nonlinear characteristics of the system. We propose the use of a parameter which governs transitions from supercritical to subcritical bifurcations as a nonlinear gain margin of the system. Results based on numerical simulations support the analytical predictions of this work.

B. MATHEMATICAL MODEL

Consider the ideal 3rd–order regulator system shown in Figure 1, where y is the actual output, $y_{\mathrm{ref}} = 0$ is the reference input, and,

$$G(s) = \frac{1}{s^3 + \alpha_2 s^2 + \alpha_1 s + \alpha_0} \, , \tag{1}$$

where the coefficients α_i correspond to a stable polynomial. In state space form, the system depicted in Figure 1 is written as,

$$\dot{x}_1 \;=\; x_2 \, , \tag{2}$$

$$\dot{x}_2 \;=\; x_3 \, , \tag{3}$$

$$\dot{x}_3 \;=\; -\alpha_2 x_3 - \alpha_1 x_2 - (\alpha_0 + K)x_1 \, , \tag{4}$$

where the state vector is,

$$x_1 = y \, , \quad x_2 = \dot{y} \, , \quad x_3 = \ddot{y} \, . \tag{5}$$

Physically, we can think of this system as a representation of the fundamental turning dynamics of a marine vehicle. In this context, x_1 represents the vehicle's lateral deviation from the commanded straight line path, x_2 is

2
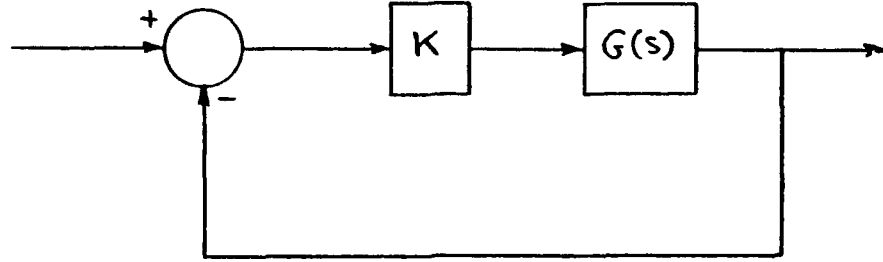
Figure 1: Ideal 3rd-order regulator system

the orientation angle, and x_3 the turning rate. To account for the geometric nonlinearities, the first state equation (2) is written as,

$$\dot{x}_1 = x_2 + \gamma x_2^3 , \qquad (6)$$

where $\gamma < 0$ for softening spring characteristics. To account for possible "over-steering" or "under-steering" effects, we modify the output of the block K of Figure 1, to

$$control \quad effort = -Ky - K_3 y^3 , \qquad (7)$$

instead of $-Ky$ of the linear element. Therefore, the nonlinear system under consideration is,

$$\begin{bmatrix} \dot{x}_1 \\ \dot{x}_2 \\ \dot{x}_3 \end{bmatrix} = \begin{bmatrix} 0 & 1 & 0 \\ 0 & 0 & 1 \\ -(\alpha_0 + K) & -\alpha_1 & -\alpha_2 \end{bmatrix} \begin{bmatrix} x_1 \\ x_2 \\ x_3 \end{bmatrix} + \begin{bmatrix} \gamma x_2^3 \\ 0 \\ -K_3 x_1^3 \end{bmatrix} . \qquad (8)$$

3

C. OUTLINE OF ANALYSIS

The following steps are performed in order to analyze system (8). First, application of Routh's criterion yields the value of the gain margin, or the critical value of K for stability. Then we rewrite the system of equations in its normal coordinate form, and use the center manifold theorem to reduce the system into a two dimensional system. We apply the method of averaging to the reduced system, and finally, we introduce polar coordinates to the averaged system in order to reveal the existence of limit cycles. Development of these computations is the subject of the next chapter.

II. ANALYSIS

A. LOSS OF STABILITY

The characteristic equation of (8) is,

$$s^3 + \alpha_2 s^2 + \alpha_1 s + (\alpha_0 + K) = 0 . \qquad (9)$$

Application of Routh's criterion to system (9) yields the critical value of K, K_c, for stability of $x_1 = x_2 = x_3 = 0$,

$$K_c = \alpha_1 \alpha_2 - \alpha_0 . \qquad (10)$$

If $K < K_c$ the system is stable, whereas for $K > K_c$ it becomes unstable. The value of K_c, given in equation (10), expressed in decibels represents the gain margin of the system.

At the critical point, $K = \alpha_1 \alpha_2 - \alpha_0$, the characteristic equation (9) is,

$$s^3 + \alpha_2 s^2 + \alpha_1 s + \alpha_1 \alpha_2 = 0 ,$$

which has roots,

$$
\begin{aligned}
s_1 &= -\sqrt{\alpha_1} i , \\
s_2 &= +\sqrt{\alpha_1} i , \qquad (11) \\
s_3 &= -\alpha_2 .
\end{aligned}
$$

Therefore, we can see that the above loss of stability is characterized by the existence of a pair of purely imaginary roots. As K crosses K_c, one pair of complex conjugate roots of (9) crosses transversally the imaginary axis.

A situation like this in which a certain parameter is varied such that the real part of one pair of complex conjugate eigenvalues of the linearized system matrix crosses zero, results in the system leaving its steady state in an oscillatory manner. This loss of stability is called Hopf bifurcation (Guckenheimer & Holmes, 1983) and generically occurs in one of two ways, supercritical or subcritical. In the supercritical case, stable limit cycles are generated after the nominal straight line motion loses its stability. The amplitudes of these limit cycles are continuously increasing as the parameter distance from its critical value is increased. For small values of this criticality distance the resulting limit cycle is of small amplitude and differs little from the initial nominal state. In the subcritical case, however, stable limit cycles are generated before the nominal state loses its stability. Therefore, depending on the initial conditions it is possible to diverge away from the nominal straight line path and converge towards a limit cycle even before the nominal motion loses its stability. This means that in the subcritical Hopf bifurcation case the domain of attraction of the nominal state is decreasing and in fact it shrinks to zero as the critical point is approached. Random external disturbances of sufficient magnitude can throw the vehicle off to an oscillatory steady state even though the nominal state may still remain stable. After the nominal state becomes unstable, a discontinuous increase in the magnitude of motions is observed as there exist no simple stable nearby attractors for the vehicle trajectory to converge to. Distinction between these two qualitatively different types of bifurcation is, therefore, essential in the

6

design of the autopilot. The computational procedure requires examination of the higher order terms in the equations of motion and it is the subject of the next section.

B. COORDINATE TRANSFORMATIONS

System (8) is written in the form,

$$\dot{\mathbf{x}} = \mathbf{A}\mathbf{x} + \mathbf{g}(\mathbf{x}) \,, \tag{12}$$

where $\mathbf{A}$ is the linearized system matrix and $\mathbf{g}(\mathbf{x})$ contains the cubic terms. At the bifurcation point $K = K_c$, matrix $\mathbf{A}$ has eigenvalues given by (11), and eigenvectors,

$$\mathbf{T} = \begin{bmatrix} 0 & 1/\sqrt{\alpha_1} & 1 \\ 1 & 0 & -\alpha_2 \\ 0 & -\sqrt{\alpha_1} & \alpha_2^2 \end{bmatrix} \,. \tag{13}$$

By taking $\mathbf{T}$ to be the matrix of critical eigenvectors of $\mathbf{A}$, the transformation,

$$\mathbf{x} = \mathbf{T}\mathbf{z} \,, \quad \mathbf{z} = \mathbf{T}^{-1}\mathbf{x} \,, \tag{14}$$

transforms system (12) into its normal coordinate form,

$$\dot{\mathbf{z}} = \mathbf{T}^{-1}\mathbf{A}\mathbf{T}\mathbf{z} + \mathbf{T}^{-1}\mathbf{g}(\mathbf{T}\mathbf{z}) \,, \tag{15}$$

where,

$$\mathbf{T}^{-1} = \frac{1}{\alpha_1 + \alpha_2^2} \begin{bmatrix} \alpha_1\alpha_2 & \alpha_1 + \alpha_2^2 & \alpha_2 \\ \sqrt{\alpha_1}\alpha_2^2 & 0 & -\sqrt{\alpha_1} \\ \alpha_1 & 0 & 1 \end{bmatrix} \,, \tag{16}$$

and,

$$\mathbf{T}^{-1}\mathbf{A}\mathbf{T} = \begin{bmatrix} 0 & -\sqrt{\alpha_1} & 0 \\ \sqrt{\alpha_1} & 0 & 0 \\ 0 & 0 & -\alpha_2 \end{bmatrix} \,. \tag{17}$$

7

For values of K close to the bifurcation point K_c, the matrix $\mathbf{T^{-1}AT}$ becomes,

$$\mathbf{T^{-1}AT} = \begin{bmatrix} \alpha'\varepsilon & -(\sqrt{\alpha_1} + \omega'\varepsilon) & 0 \\ \sqrt{\alpha_1} + \omega'\varepsilon & \alpha'\varepsilon & 0 \\ 0 & 0 & -\alpha_2 + p'\varepsilon \end{bmatrix} ,$$

where ε denotes the criticality difference,

$$\varepsilon = K - K_c , \qquad (19)$$

and α' is the derivative of the real part of the critical eigenvalues with respect to ε, ω' is the derivative of the imaginary part of the critical eigenvalues with respect to ε, and p' is the derivative of the third eigenvalue s_3 with respect to ε. These are computed using a perturbation series approach as follows. The characteristic equation (9) can be written in the form,

$$s^3 + \alpha_2 s^2 + \alpha_1 s + (\alpha_1 \alpha_2 + \varepsilon) = 0 , \qquad (20)$$

where we have used (10) and (19). The roots of (20) are expressed as,

$$s_1 = \alpha'\varepsilon - (\sqrt{\alpha_1} + \omega'\varepsilon) i , \qquad (21)$$

$$s_2 = \alpha'\varepsilon + (\sqrt{\alpha_1} + \omega'\varepsilon) i , \qquad (22)$$

$$s_3 = -\alpha_2 + p'\varepsilon . \qquad (23)$$

If we substitute (21) through (23) in (20) and neglect terms of order ε^2, ε^3, we get,

$$\alpha' = \frac{1}{2(\alpha_1 + \alpha_2^2)} , \qquad (24)$$

$$\omega' = \frac{\alpha_2}{2\sqrt{\alpha_1}(\alpha_1 + \alpha_2^2)} , \qquad (25)$$

$$p' = -\frac{1}{\alpha_1 + \alpha_2^2} . \qquad (26)$$

8

C. REDUCTION OF ORDER

The physical variables x_i are related to the normal coordinates z_i through (14), and using (13) we get,

$$
\begin{aligned}
x_1 &= \frac{1}{\sqrt{\alpha_1}} z_2 + z_3 \ , \\
x_2 &= z_1 - \alpha_2 z_3 \ , \\
x_3 &= -\sqrt{\alpha_1} z_2 + \alpha_2^2 z_3 \ .
\end{aligned}
\tag{27}
$$

It can be seen from (26) that $p' < 0$, and therefore the eigenvalue s_3 is locally (for ϵ small) negative, as shown in equation (23). In fact, a quick root locus plot of (9) will show that s_3 is negative for all values of $K > 0$. Therefore, the flow of (8) in the direction of z_3 converges to zero. All interesting bifurcation phenomena are locally restricted on a two dimensional manifold that decsribes the time evolution of the critical coordinates z_1, z_2; this is the center manifold of (8). According to the center manifold theorem (Guckenheimer & Holmes, 1983), the stable coordinate z_3 can be expressed as a function of the critical coordinates z_1, z_2, and this relationship is at least of quadratic order. In fact due to the symmetry in our problem, the above relationship is of third order. Therefore, z_3 does not affect the nonlinear terms in (15) and we can write (27) in the form,

$$
\begin{aligned}
x_1 &= \frac{1}{\sqrt{\alpha_1}} z_2 \ , \\
x_2 &= z_1 \ , \\
x_3 &= -\sqrt{\alpha_1} z_2 \ .
\end{aligned}
\tag{28}
$$

9

Using (28) we can write,

$$\mathbf{g(Tz)} = \begin{bmatrix} \gamma z_1^3 \\ 0 \\ -K_3 z_2^3/\alpha_1^{3/2} \end{bmatrix} ,$$

and,

$$\mathbf{T^{-1}g(Tz)} = \frac{1}{\alpha_1 + \alpha_2^2} \begin{bmatrix} \alpha_1\alpha_2\gamma z_1^3 - K_3 z_2^3 \alpha_2/\alpha_1^{3/2} \\ \sqrt{\alpha_1}\alpha_2^2\gamma z_1^3 + K_3 z_2^3/\alpha_1 \\ \alpha_1\gamma z_1^3 - K_3 z_2^3/\alpha_1^{3/2} \end{bmatrix} . \qquad (29)$$

Using equations (18) and (29) we substitute in (15) and write the normal equations in z_1, z_2 as,

$$\dot{z}_1 = \alpha'\epsilon z_1 - (\sqrt{\alpha_1} + \omega'\epsilon)z_2 + F_1(z_1, z_2) , \qquad (30)$$

$$\dot{z}_2 = (\sqrt{\alpha_1} + \omega'\epsilon)z_1 + \alpha'\epsilon z_2 + F_2(z_1, z_2) , \qquad (31)$$

where,

$$F_1(z_1, z_2) = \frac{\alpha_1\alpha_2}{\alpha_1 + \alpha_2^2}\gamma z_1^3 - \frac{\alpha_2}{(\alpha_1 + \alpha_2^2)\alpha_1^{3/2}}K_3 z_2^3 , \qquad (32)$$

$$F_2(z_1, z_2) = \frac{\sqrt{\alpha_1}\alpha_2^2}{\alpha_1 + \alpha_2^2}\gamma z_1^3 + \frac{1}{(\alpha_1 + \alpha_2^2)\alpha_1}K_3 z_2^3 . \qquad (33)$$

Equations (30) and (31) describe the suspended center manifold flow of (15) (Guckenheimer & Holmes, 1983).

D. AVERAGING

If we introduce polar coordinates in the form,

$$z_1 = R\cos\theta , \quad z_2 = R\sin\theta , \qquad (34)$$

10

we can write equations (30), (31) as,

$$\dot{R} = \alpha'\epsilon R + F_1(R\cos\theta, R\sin\theta)\cos\theta$$

$$+ F_2(R\cos\theta, R\sin\theta)\sin\theta , \qquad (35)$$

$$R\dot{\theta} = (\sqrt{\alpha_1} + \omega'\epsilon)R + F_2(R\cos\theta, R\sin\theta)\cos\theta$$

$$- F_1(R\cos\theta, R\sin\theta)\sin\theta . \qquad (36)$$

Equation (35) is written in the form,

$$\dot{R} = \alpha'\epsilon R + \mathcal{P}(\theta)R^3 , \qquad (37)$$

where the function $\mathcal{P}(\theta)$ is 2π–periodic in the angular coordinate θ,

$$\mathcal{P}(\theta) = \frac{\alpha_1\alpha_2}{\alpha_1 + \alpha_2^2}\gamma\cos^4\theta - \frac{\alpha_2}{(\alpha_1 + \alpha_2^2)\alpha_1^{3/2}}K_3\cos\theta\sin^3\theta$$

$$+ \frac{\sqrt{\alpha_1}\alpha_2^2}{\alpha_1 + \alpha_2^2}\gamma\cos^3\theta\sin\theta + \frac{1}{\alpha_1(\alpha_1 + \alpha_2^2)}K_3\sin^4\theta . \qquad (38)$$

If equation (37) is averaged over one cycle in θ, we get an equation with constant coefficients,

$$\dot{R} = \alpha'\epsilon R + QR^3 , \qquad (39)$$

where

$$Q = \frac{1}{2\pi}\int_0^{2\pi}\mathcal{P}(\theta)\,d\theta . \qquad (40)$$

Substituting (38) into (40) and evaluating the integral yields,

$$Q = \frac{3}{8} \cdot \frac{\alpha_1^2\alpha_2\gamma + K_3}{\alpha_1(\alpha_1 + \alpha_2^2)} . \qquad (41)$$

Similar averaging can be performed for equation (36) which has the form,

$$\dot{\theta} = \sqrt{\alpha_1} + \omega'\epsilon + \mathcal{F}(\theta)R^2 , \qquad (42)$$

11

where --

$$\mathcal{F}(\theta) = \frac{\sqrt{\alpha_1}\,\alpha_2^2}{\alpha_1 + \alpha_2^2}\gamma\cos^4\theta + \frac{1}{\alpha_1(\alpha_1 + \alpha_2^2)}K_3\cos\theta\sin^3\theta$$

$$-\frac{\alpha_1\alpha_2}{\alpha_1 + \alpha_2^2}\gamma\cos^3\theta\sin\theta + \frac{\alpha_2}{\alpha_1^{3/2}(\alpha_1 + \alpha_2^2)}K_3\sin^4\theta \,, \quad (43)$$

and we have assumed $R \neq 0$. The averaged form of (42) is,

$$\dot{\theta} = \sqrt{\alpha_1} + \omega'\epsilon + \mathcal{G}R^2 \,, \qquad (44)$$

where

$$\mathcal{G} = \frac{1}{2\pi}\int_0^{2\pi}\mathcal{F}(\theta)\,d\theta \,, \qquad (45)$$

and using (43),

$$\mathcal{G} = \frac{3\alpha_2}{8}\cdot\frac{\alpha_1^2\alpha_2\gamma - K_3}{\alpha_1^{3/2}(\alpha_1 + \alpha_2^2)} \,. \qquad (46)$$

The system of equations (39) and (44) exhibits similar stability properties to the original system (37) and (42) (Chow & Mallet–Paret, 1977), and is studied in the following section.

E. LIMIT CYCLE ANALYSIS

Equation (39) has two steady state solutions, one at $R = 0$ which corresponds to the trivial equilibrium solution at zero, and one at

$$R_0^2 = -\frac{\alpha'}{\mathcal{Q}}\epsilon \,. \qquad (47)$$

This equilibrium solution corresponds to a periodic solution or limit cycle in the cartesian coordinates z_1, z_2 from (64). Since α' as seen by (24) is

12

always positive, existence of these periodic solutions depends on the value of Q. Specifically,

- if $Q < 0$, periodic solutions exist for $\epsilon > 0$ or $K > K_c$, and

- if $Q > 0$, periodic solutions exist for $\epsilon < 0$ or $K < K_c$.

The Floquét exponent of (39) in the vicinity of (47) is

$$\beta = -2\alpha'\epsilon , \qquad (48)$$

and we can see that

- if periodic solutions exist for $K > K_c$ they are stable, and

- if periodic solutions exist for $K < K_c$ they are unstable.

We refer to the first case as the supercritical Poincaré–Andronov–Hopf (PAH) bifurcation and to the second case as the subcritical PAH bifurcation (Guckenheimer & Holmes, 1983).

The period of these limit cycles is computed by substituting (47) in (44),

$$T = \frac{2\pi}{\sqrt{\alpha_1 + \omega'\epsilon + \mathcal{G}R_0^2}} = \frac{2\pi}{\sqrt{\alpha_1}}\left(1 - \frac{\omega'Q - \alpha'\mathcal{G}}{\sqrt{\alpha_1}Q}\epsilon\right) + O(\epsilon^2) . \qquad (49)$$

The amplitude of the limit cycles is computed from (47) and (28), and in terms of the physical variables x_1, x_2, x_3, we get,

$$x_1 = 2\frac{\sqrt{3}}{3}\sqrt{\frac{\alpha_1\alpha_2 - \alpha_0 - K}{\alpha_1^2\alpha_2\gamma + K_3}} , \qquad (50)$$

$$x_2 = 2\frac{\sqrt{3}}{3}\sqrt{\frac{\alpha_1(\alpha_1\alpha_2 - \alpha_0 - K)}{\alpha_1^2\alpha_2\gamma + K_3}} , \qquad (51)$$

13

$$x_3 = 2\alpha_1 \frac{\sqrt{3}}{3} \sqrt{\frac{\alpha_1 \alpha_2 - \alpha_0 - K}{\alpha_1^2 \alpha_2 \gamma + K_3}} \,. \tag{52}$$

We can see that in the supercritical case, on loss of stability of equilibrium the steady state becomes a periodic oscillatory state, the amplitude of the oscillation being proportional to the square root of the criticality ϵ, the difference of the gain K from its critical value K_c at which stability of equilibrium is lost. This form of loss of stability is called "soft" loss of stability since the oscillating state for small ϵ differs little from the equilibrium state. In the subcritical case, before the steady state loses stability the domain of attraction becomes very small as is bounded by the amplitudes of the unstable limit cycles, and a random disturbance can throw the system off its equilibrium state even before its domain of attraction has completely disappeared. This form of loss of stability is called "hard". Here the system leaves its steady state with a jump to a different state of motion which can be a stable oscillation with a locally discontinuous increase in the amplitude, a more complicated bounded motion, or even an unbounded motion depending on other higher–than–third order terms that have not been incorporated in system (8).

III. RESULTS AND DISCUSSION

A. RESULTS

For demonstration purposes we assume that in the case $K = 0$ the system has been designed in accordance to the ITAE optimal criterion for third order systems; i.e.,

$$\alpha_2 = 1.75\omega_n$$
$$\alpha_1 = 2.15\omega_n^2 , \tag{53}$$
$$\alpha_0 = \omega_n^3 ,$$

where the natural frequency ω_n is in general selected according to the desired bandwidth of the system. The ITAE criterion is a standard performance index and it minimizes the integral time absolute error $\int_0^\infty t|e(t)|\,dt$, of the step response $e(t)$ of a system (Dorf, 1992). This criterion is satisfied for a third order system when the coefficients of its characteristic equation are selected as in equations (53). The critical value of K for stability is computed by,

$$K_c = \alpha_1\alpha_2 - \alpha_0 = 2.7625\omega_n^3 . \tag{54}$$

A graphical representation of equation (54) is shown in Figure 2 for a nominal range of ω_n between 1 and 2 rad/sec.

The cubic coefficient Q that dictates the nature (supercritical or subcritical) and stability of the resulting limit cycles as K exceeds K_c is given by
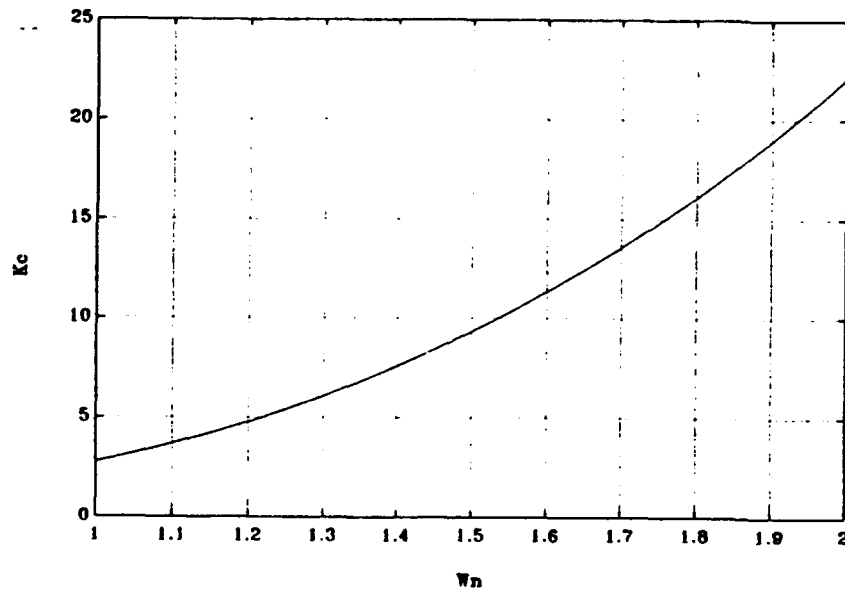
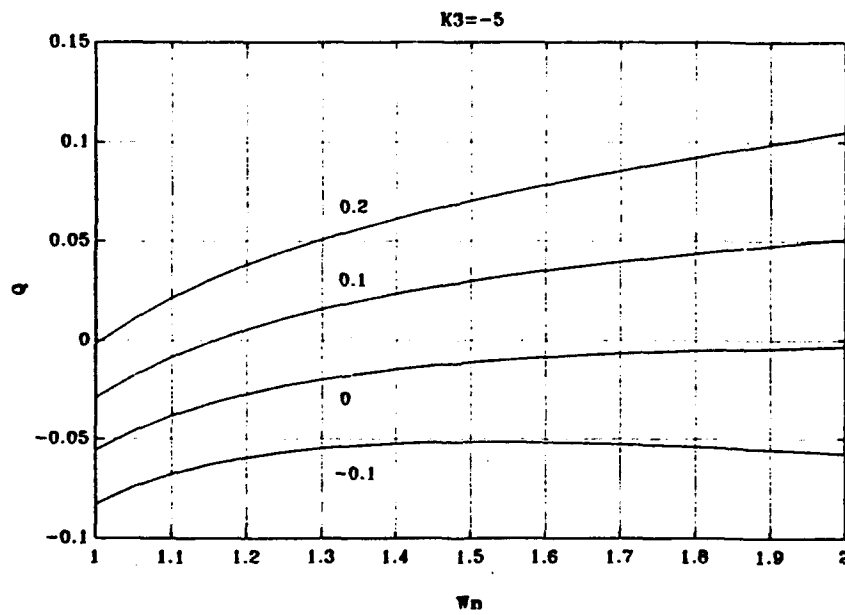Figure 2: Critical value K_c versus ω_n

Figure 3: Cubic coefficient Q versus ω_n for $K_3 = -5$ and different values of γ

16

(41), and using (53) we get,

$$Q = 0.2707\omega_n\gamma + 0.0112\frac{K_3}{\omega_n^4} \,. \tag{55}$$

A plot of equation (55) for $K_3 = -5$ and four different values of γ is shown in Figure 3.

Based on the results presented in Figure 3, the following observations can be made: (1) For fixed K_3 and a given value of ω_n, supercritical bifurcations are ensured for a value of γ less than a critical threshold, computed by equating $Q = 0$. (2) In the case of supercritical bifurcations, we expect to see an oscillatory response approaching zero when $K < K_c$ and converging to a periodic solution for $K > K_c$. The above response should be independent of the initial conditions, at least locally. (3) In the case of subcritical bifurcations, we expect to see an oscillatory response for $K < K_c$ which may or may not converge to zero. This depends on the initial conditions. If the response diverges from zero, the final attractor can be another oscillation or a more complicated motion. The same is true for $K > K_c$, here the response should diverge regardless of the initial conditions. These conclusions are confirmed in the next section using direct numerical integrations of equations (8).

B. NUMERICAL SIMULATIONS

An example of supercritical behavior is shown in Figures 4 and 5. In both of these figures we present results based on direct numerical integrations of

equations (8) for the following conditions,

$$\omega_n = 2 \ , \quad K = 1.05 K_c \ , \quad K_3 = -5 \ , \quad \gamma = -0.1 \ . \qquad (56)$$

For these conditions, which are selected to demonstrate the supercritical case, we can see from Figure 3 that $Q < 0$ and, therefore, we have a supercritical Hopf bifurcation. Figure 4 shows clearly the development of a stable periodic solution with amplitude $x_2 = 0.68$ and period $T = 2.14$. The theoretical value for the limit cycle amplitude is computed from (56) and (51), as $x_2 = 0.6405$ which is in excellent agreement with the numerical value. Likewise, the period of oscillation is found from (56) and (49), as $T = 2.1351$ which is also close to the actual period. Figure 5 shows the convergence to the limit cycle in the $(x_2, \dot{x}_2)$ phase subspace using two sets of initial conditions. One set $(x_1, x_2, x_3) = (0, 0.5, 0)$ is located inside the limit cycle and the other set $(x_1, x_2, x_3) = (0, 1, 0)$ is located outside the limit cycle. It can be seen that both trajectories converge to the, numerically computed, periodic solution.

An example of subcritical behavior for $K > K_c$ is shown in Figures 6 and 7. In both of these figures the conditions were the same as (56) with the exception of γ which was $\gamma = 0.2$ for Figure 6 and $\gamma = 0.1$ for Figure 7. These correspond to $Q > 0$ as can be seen from Figure 3, which confirms the subcritical behavior. The motion which corresponds to $\gamma = 0.2$ is strongly subcritical and it becomes unbounded shortly after 20 seconds. The motion which corresponds to $\gamma = 0.1$ is less subcritical since it yields a smaller, but still positive, value for Q. As seen in Figure 7, it appears that trajectories
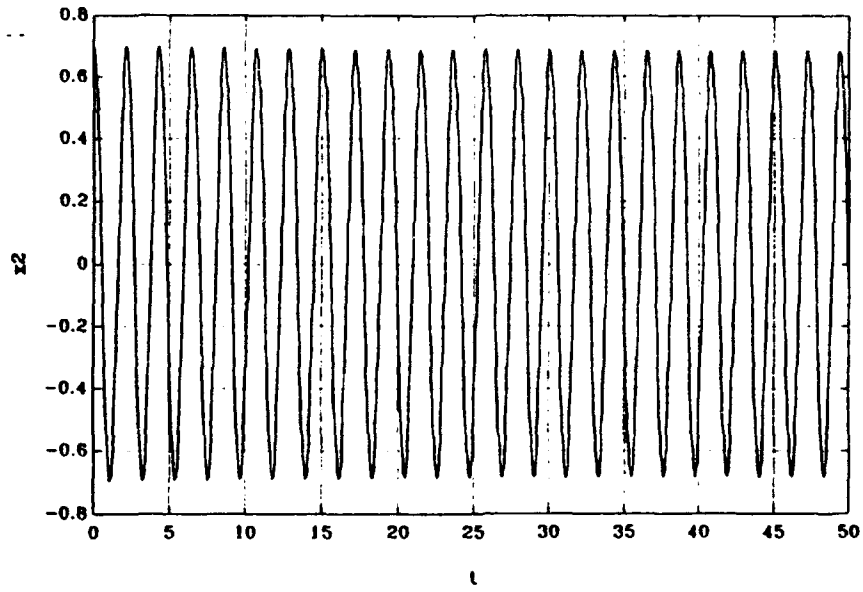
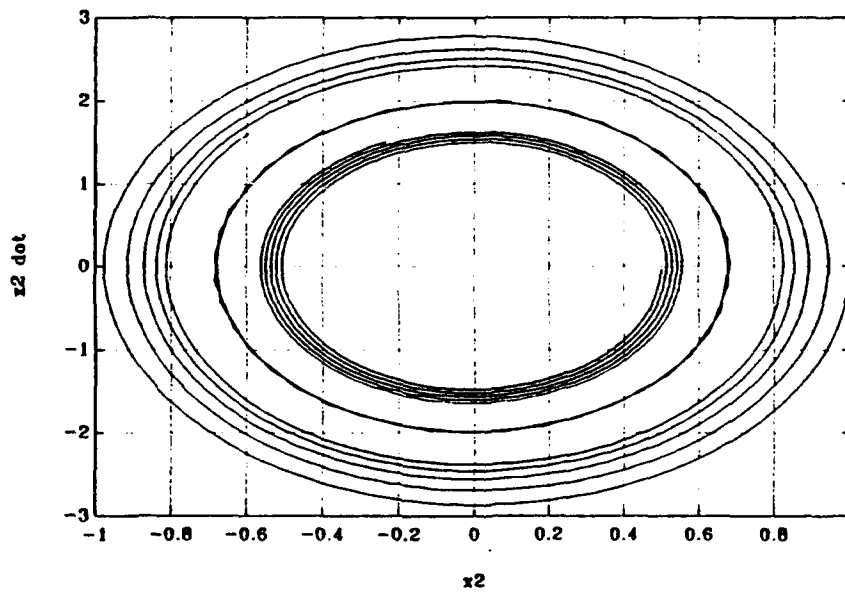Figure 4: Time history (t, x_2) for $\omega_n = 2$, $K = 1.05 K_c$, $K_3 = -5$, and $\gamma = -0.1$

Figure 5: Phase subspace plot $(x_2, \dot{x}_2)$ for $\omega_n = 2$, $K = 1.05 K_c$, $K_3 = -5$, $\gamma = -0.1$, and two initial conditions

19
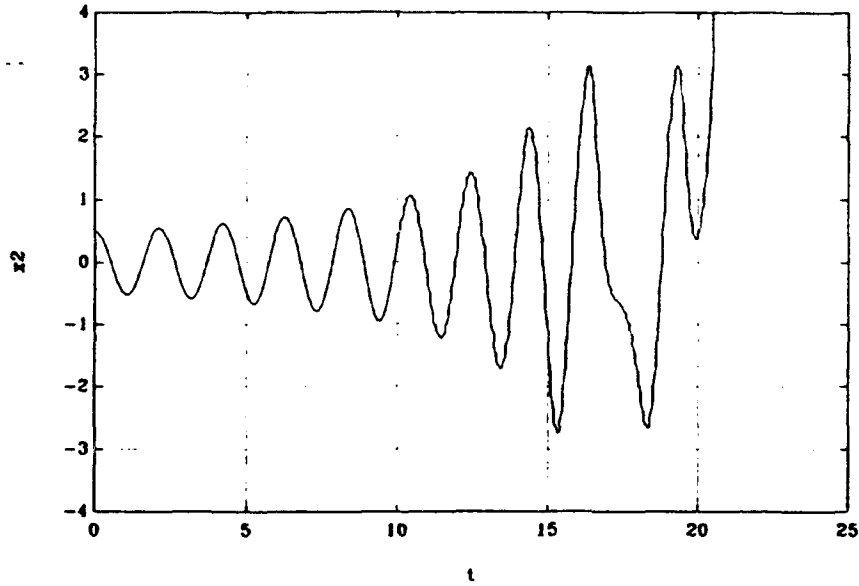
Figure 6: Time history (t, x_2) for $\omega_n = 2$, $K = 1.05 K_c$, $K_3 = -5$, and $\gamma = 0.2$

converge to a relaxation oscillation of high amplitude.

An example of subcritical behavior for $K < K_c$ is shown in Figures 8 and 9, for the following conditions,

$$\omega_n = 2 , \quad K = 0.95 K_c , \quad K_3 = -5 , \quad \gamma = 0.2 , \tag{57}$$

and different initial conditions in x_2. For small initial conditions, $(x_1, x_2, x_3) = (0, 0.1, 0)$, the system is located inside the unstable limit cycle and it converges to the stable equilibrium, as shown in Figure 8. However, for large initial conditions, $(x_1, x_2, x_3) = (0, 0.5, 0)$, the system trajectory is located outside the unstable limit cycle and it diverges away from the equilibrium, even though this equilibrium is still stable. It appears from Figure 9 that, for small γ, the system converges to a relaxation oscillation, while higher value
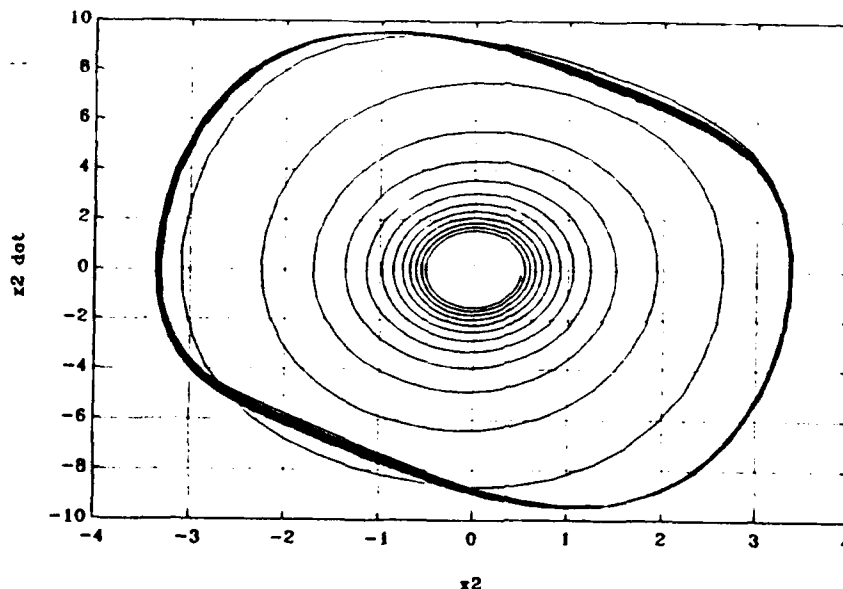
20

Figure 7: Phase subspace plot $(x_2, \dot{x}_2)$ for $\omega_n = 2$, $K = 1.05 K_c$, $K_3 = -5$, and $\gamma = 0.1$

of γ generate more severe subcritical behavior and the motion becomes unbounded, as before. In the case of supercritical behavior and for $\acute{K} < K_c$, we observed that numerical integrations converged to the stable equilibrium regardless of the initial condition in x_2, as they should.

C. MULTIPLE EQUILIBRIUM STATES

So far, our analysis has been on stability properties of the trivial equilibrium of (8), and its bifurcations to periodic solutions. It is possible, however, that additional equilibrium points may exist. To explore this, we write sys-
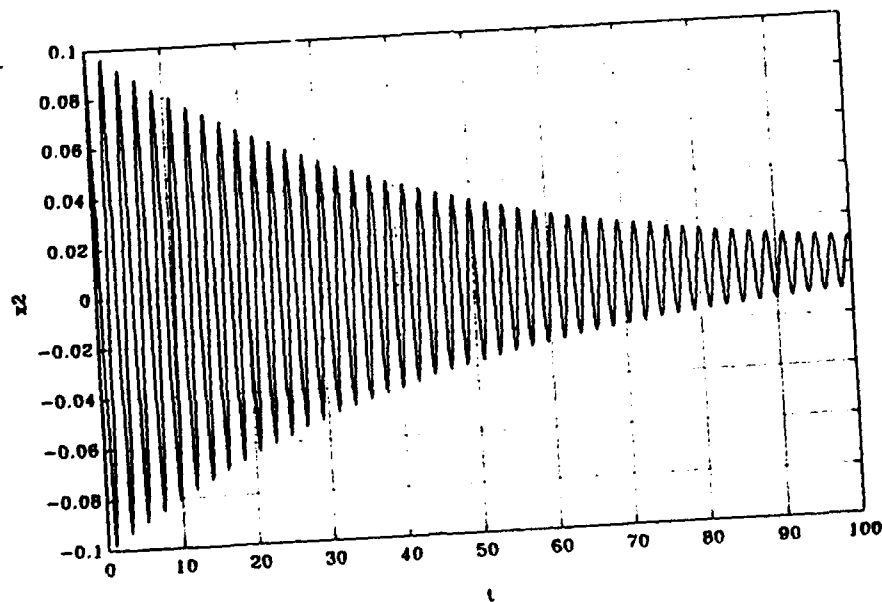
21

Figure 8: Time history (t, x_2) for $\omega_n = 2$, $K = 0.95 K_c$, $K_3 = -5$, $\gamma = 0.2$, and $x_2(t = 0) = 0.1$
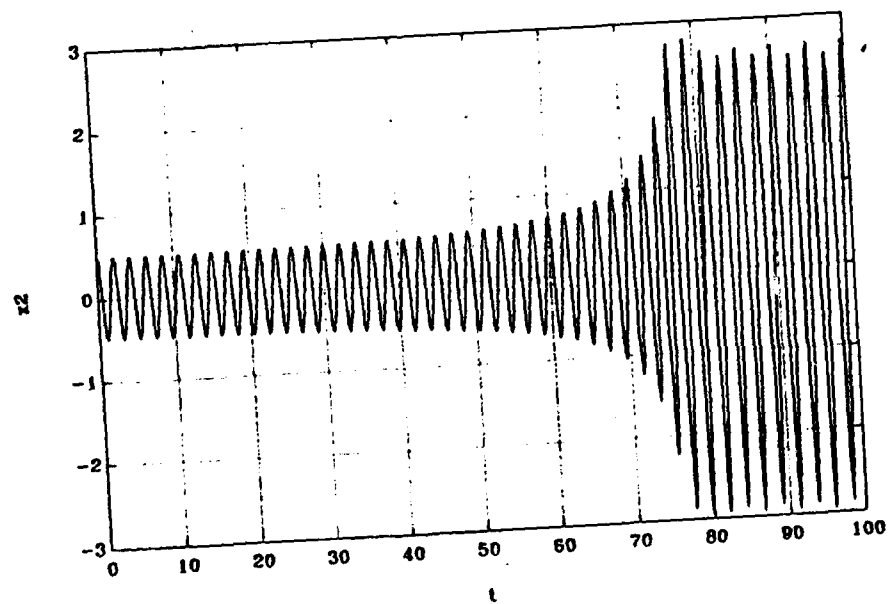

Figure 9: Time history (t, x_2) for $\omega_n = 2$, $K = 0.95 K_c$, $K_3 = -5$, $\gamma = 0.2$, and $x_2(t = 0) = 0.5$
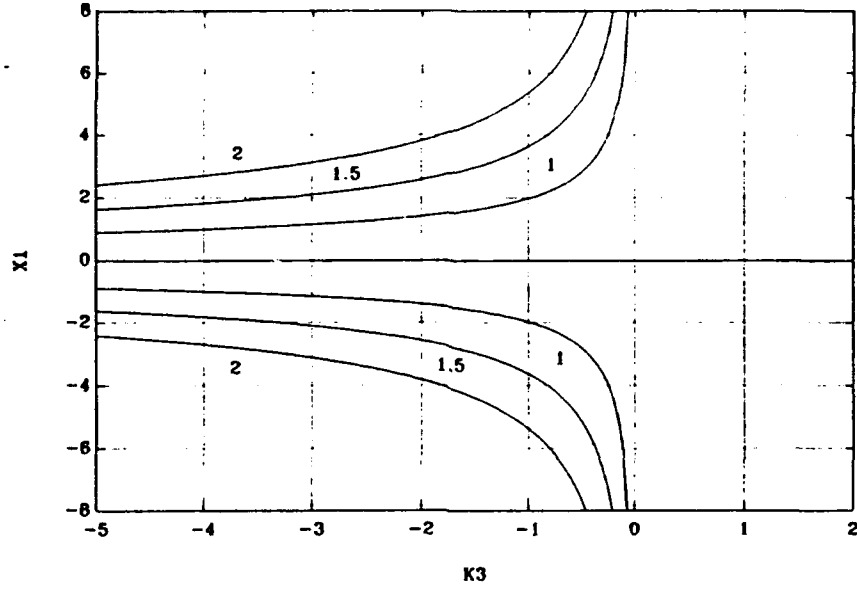
22

Figure 10: Steady state solutions X_1 versus K_3 for $K = 0.95K_c$, $\gamma = 0$, and three values of ω_n

tem (8) in the form,

$$\dot{x}_1 = x_2 + \gamma x_2^3 , \tag{58}$$

$$\dot{x}_2 = x_3 , \tag{59}$$

$$\dot{x}_3 = -(\alpha_0 + K)x_1 - \alpha_1 x_2 - \alpha_2 x_3 - K_3 x_1^3 . \tag{60}$$

In order to compute its equilibrium points we must set the time derivatives $\dot{x}_1$, $\dot{x}_2$, $\dot{x}_3$ zero, and solve for the equilibrium point X_1, X_2, X_3. We examine the case $\gamma \geq 0$ first.

Equation (58) yields,

$$X_2 + \gamma X_2^3 = 0 , \tag{61}$$

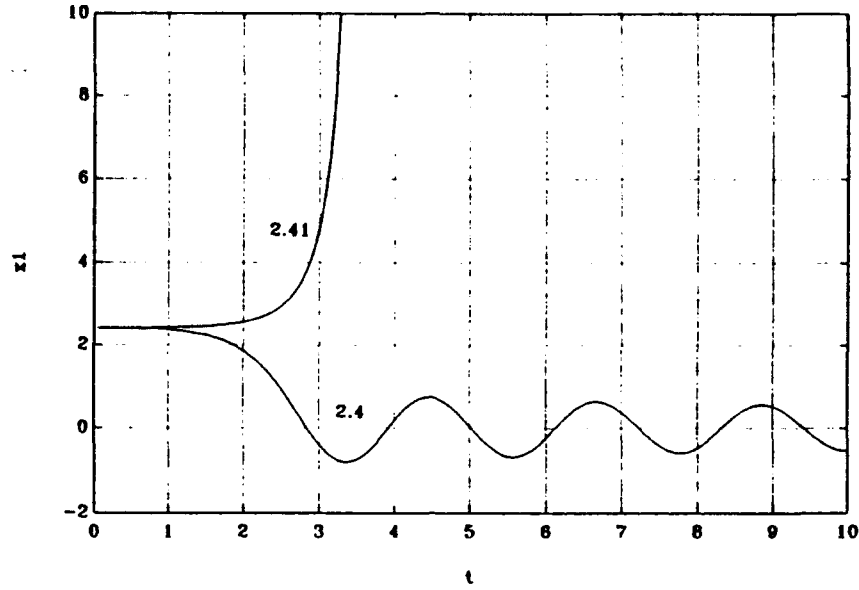which, since $\gamma \geq 0$, has only one solution, namely $X_2 = 0$. Equation (59)

23

Figure 11: Time history (t, x_1) for $\omega_n = 2$, $K = 0.95K_c$, $K_3 = -5$, $\gamma = 0$, and two initial conditions in x_1

gives $X_3 = 0$, and then (60) can be solved for the remaining equilibrium solution X_1,

$$X_1(\alpha_0 + K + K_3 X_1^2) = 0 . \tag{62}$$

Equation (62) admits the trivial solution, $X_1 = 0$, always, and two more possible solutions provided $K_3 < 0$, given by,

$$X_1^2 = -\frac{\alpha_0 + K}{K_3} . \tag{63}$$

Equation (63) yields two additional symmetrically located equilibrium points which are generated as K_3 becomes negative. A typical plot for $K = 0.95K_c$ and three values of $\omega_n = 1$, 1.5, 2 is presented in Figure 10. Therefore, we see that the same coefficient, K_3, which governs the transition from subcritical

24

to supercritical bifurcations to periodic solutions of the trivial equilibrium state, is also associated with the existence of additional equilibrium states.

In order to analyze the stability properties of these solutions we linearize equations (58) through (60) in the neighborhood of X_i. If we denote by ξ_i the deviation of x_i from equilibrium; i.e, $\xi_i = x_i - X_i$, we can write the linearized system as,

$$
\begin{aligned}
\dot{\xi_1} &= \xi_2 \,, \\
\dot{\xi_2} &= \xi_3 \,, \\
\dot{\xi_3} &= -(\alpha_0 + K)\xi_1 - \alpha_1\xi_2 - \alpha_2\xi_3 - 3K_3 X_1^2 \xi_1 \,.
\end{aligned}
\tag{64}
$$

If we substitute (63) in (64) we get,

$$
\begin{aligned}
\dot{\xi_1} &= \xi_2 \,, \\
\dot{\xi_2} &= \xi_3 \,, \\
\dot{\xi_3} &= 2(\alpha_0 + K)\xi_1 - \alpha_1\xi_2 - \alpha_2\xi_3 \,.
\end{aligned}
\tag{65}
$$

The characteristic equation of (65) is,

$$
s^3 + \alpha_2 s^2 + \alpha_1 s - 2(\alpha_0 + K) = 0 \,,
\tag{66}
$$

which means that the additional non–trivial equilibria are clearly unstable with divergent dynamics. Therefore, the case $K_3 < 0$ which was shown to be beneficial from the point of view of Hopf bifurcations, is undesirable from the point of view of static bifurcations. The final compromise depends of course on the particular demands and specifications of the design. Figure 11
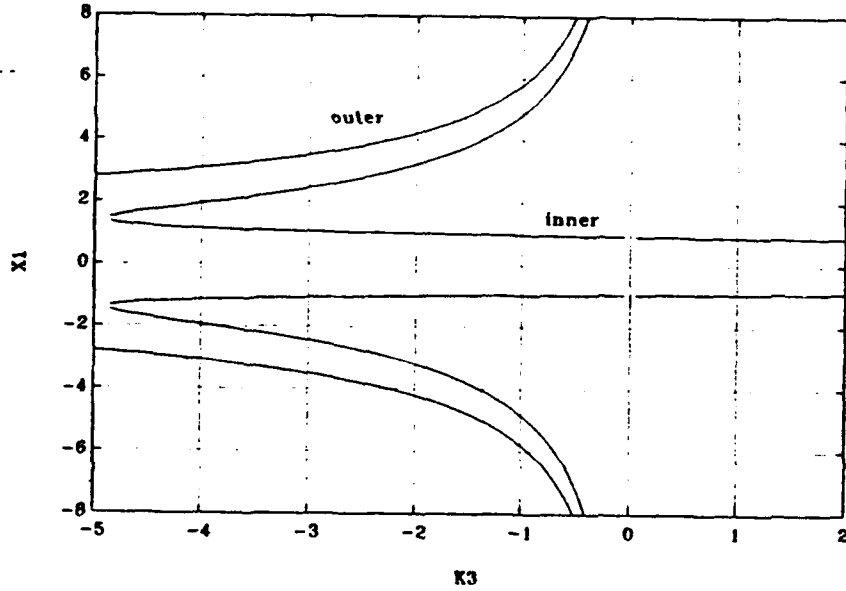
Figure 12: Steady state solutions X_1 versus K_3 for $K = 0.95K_c$, $\gamma = -0.1$, $\omega_n = 2$, and $X_2 \neq 0$

demonstrates the divergent properties of the additional equilibrium states for $K_3 < 0$. Two numerical simulations (t, x_1) are shown for $K_3' = -5$, $\omega_n = 2$, and $K = 0.95K_c$, and for two sets of initial conditions, $(x_1, x_2, x_3) = (2.40, 0, 0)$ and $(x_1, x_2, x_3) = (2.41, 0, 0)$. The unstable equilibrium X_1 is located at 2.408 as predicted by (63). We can see that, as expected, numerical simulations inside the stable potential well, $x_1 < X_1$, converge to zero while those outside, $x_1 > X_1$, diverge and quickly become unbounded.

The case $\gamma < 0$ can be analyzed similarly. Equation (61) admits in this case the trivial solution $X_2 = 0$ which was analyzed previously, and two more
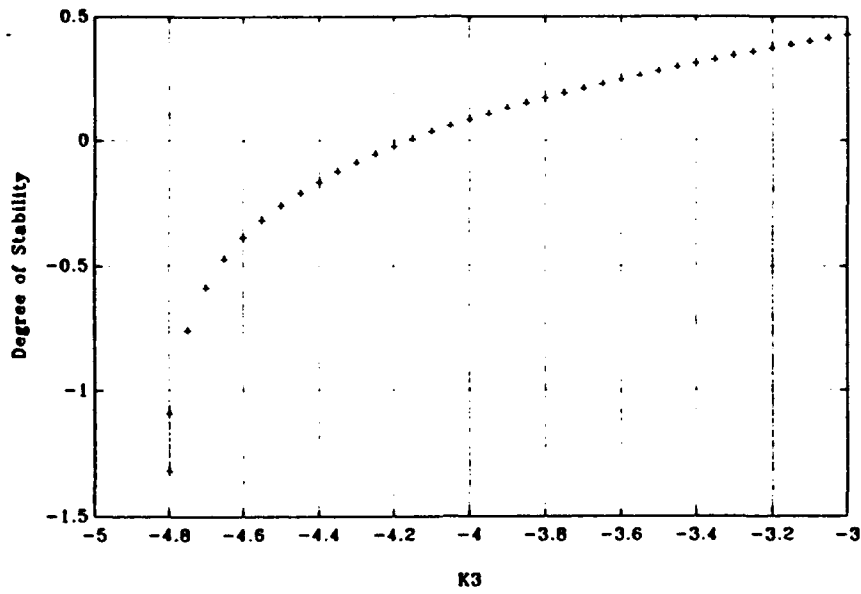
26

Figure 13: Degree of stability of the lower outer solutions which appear in Figure 12
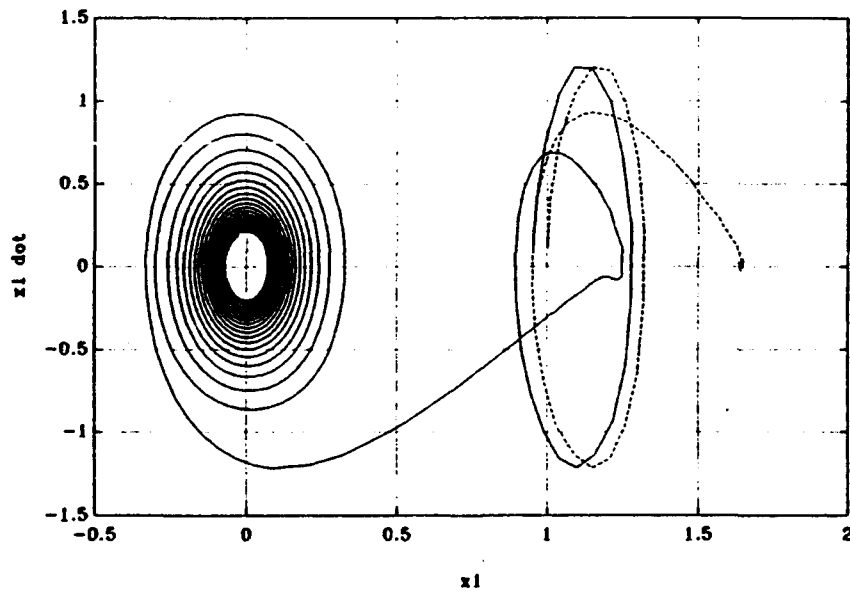

Figure 14: Trajectories for $K_3 = -4.6$ and two different initial conditions; variables correspond to Figure 12
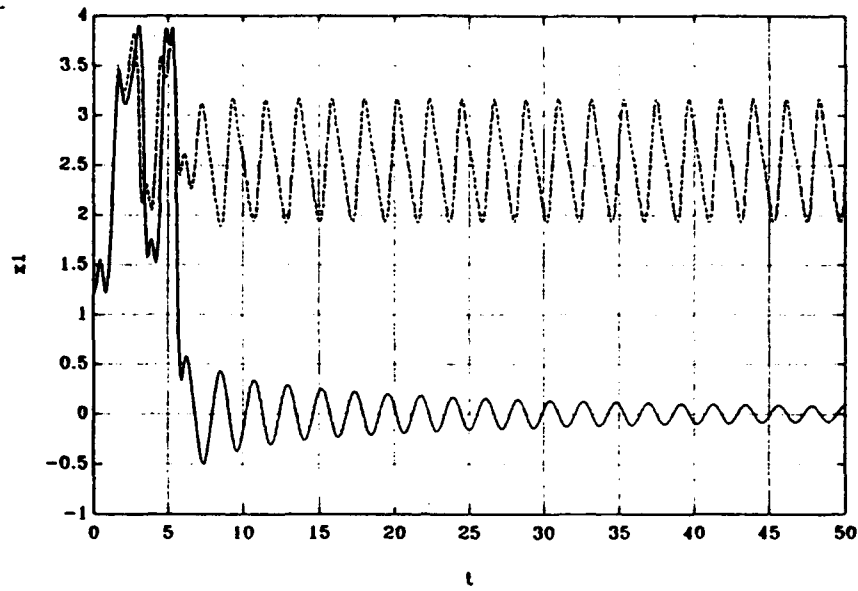
Figure 15: Time history (t, x_1) for $K_3 = -3$ and two initial conditions; variables correspond to Figure 12
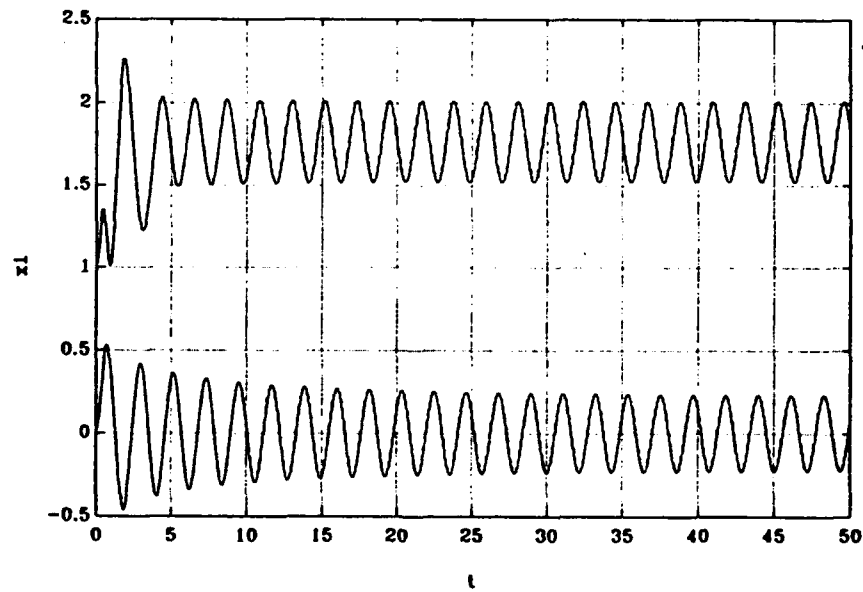

Figure 16: Time history (t, x_1) for $\omega_n = 2$, $K = 1.05K_c$, $K_3 = -5$, $\gamma = -0.1$, and two initial conditions in x_1

28

symmetrically located solutions,

$$X_2^2 = -\frac{1}{\gamma} \, . \tag{67}$$

Then $X_3 = 0$ while X_1 is obtained from (60) as the solution to,

$$(\alpha_0 + K)X_1 + \alpha_1 X_2 + K_3 X_1^3 = 0 \, . \tag{68}$$

A typical solution set of (68) is presented in Figure 12 for $\omega_n = 2$, $K = 0.95K_c$, and $\gamma = -0.1$ with X_2 given from (67). If we compare this to the corresponding solutions for $\gamma = 0$ shown in Figure 10 we can observe that the nontrivial solutions for $\gamma = 0$ retain their shape, these are denoted by outer in Figure 12. The main difference here is the existence of two outer solutions for most of the range of K_3. The trivial solution $X_1 = 0$ of Figure 10 perturbs in this case into the solution labeled as inner in Figure 12. It can also be observed that there is a point, in this case at about $K_3 = -4.8$ where the lower outer solution coalesces with the inner solution. For values of K_3 less than this critical point only the upper outer solution remains.

Stability properties of these solutions can be established by linearization. The linearized system of (58) through (60) for $X_2 \neq 0$ takes the form,

$$
\begin{aligned}
\dot{\xi}_1 &= -2\xi_2 \, , \\
\dot{\xi}_2 &= \xi_3 \, , \\
\dot{\xi}_3 &= -(\alpha_0 + K + 3K_3 X_1^2)\xi_1 - \alpha_1 \xi_2 - \alpha_2 \xi_3 \, .
\end{aligned}
\tag{69}
$$

The characteristic equation of (69) is,

$$s^3 + \alpha_2 s^2 + \alpha_1 s - 2(\alpha_0 + K + 3K_3 X_1^2) \, . \tag{70}$$

Numerical computation of the roots of (70) revealed that both the inner solution and the upper outer solutions were unstable. The lower inner solution is initially stable, in other words the point where the lower outer and the inner solutions of Figure 12 meet is a saddle–node point. The degree of stability of the lower outer solution, defined as the largest real part of the three roots of (70), is plotted in Figure 13 versus K_3. This corresponds to a complex conjugate root. We can see that it is initially stable and that it undergoes a Hopf bifurcation at a value of K_3 approximately −4.15.

These results are confirmed by the numerical integrations presented in Figures 14 through 16. For $K_3 = -4.6$, the lower outer equilibrium solution is stable. Therefore, the numerical simulations will converge to either this solution or the trivial equilibrium depending on the initial conditions, see Figure 14. The trivial equilibrium is a rather weak attractor in this case since K is very near its critical value K_c. For $K_3 = -3$, the lower outer equilibrium point has become unstable and is surrounded by a stable limit cycle. Depending on the initial conditions, trajectories will converge to either the stable trivial equilibrium or one of the two stable limit cycles, see Figure 15. Apparently there exists a region where the final outcome is sensitive to the choice of initial conditions, and the corresponding transient response resembles a random pre–chaotic motion before the trajectories converge to the corresponding attractor. This limit cycle persists as K exceeds K_c, see Figure 16. In this case the trajectories will converge to either the trivial or the non–trivial limit cycles, depending again on the initial conditions.

-IV. CONCLUSIONS AND RECOMMENDATIONS

This work presented a methodology for assessing the dynamic response of a third order system with respect to changes in its gain. Choice for the baseline system was motivated by modeling the fundamental dynamics of an autonomous vehicle. The methods, however, are of general nature and can be applied to any given system. An extensive study of the dynamic loss of stability was performed based on Hopf bifurcation theory techniques. The existence of both subcritical and supercritical bifurcations to periodic solutions was established depending on the system parameters. It was shown that the critical system gain for stability is useful for design purposes only to the extent that it is accompanied by supercritical bifurcations. The latter can be studied using a comprehensive nonlinear study like the one presented in this work. Future work should concentrate on classifying the nonlinear dynamics of various dynamical systems in terms of their order and linear/nonlinear properties. Such a generalization could allow the establishment of a more reliable set of measures than the linear gain margin, which would be used in control system design.

LIST OF REFERENCES

1. Chow, S.-N. and Mallet-Paret, J. (1977), "Integral averaging and bifurcation," *Journal of Differential Equations*, **26**, pp. 112–159.

2. Dorf, R. C. (1992), *Modern Control Systems*, Addison–Wesley.

3. Friedland, B. (1986), *Control System Design: An Introduction to State-Space Methods*, McGraw Hill, New York.

4. Guckenheimer, J. and Holmes P. (1983), *Nonlinear Oscillations, Dynamical Systems, and Bifurcations of Vector Fields*, Applied Mathematical Sciences 42, Springer–Verlag, New York.

5. Oral, Z. O. (1993), "Hopf Bifurcations in Path Control of Marine Vehicles", M.S. Thesis, Department of Mechanical Engineering, Naval Postgraduate School, Monterey, California.

INITIAL DISTRIBUTION LIST

No. Copies

1. Defense Technical Information Center   2
   Cameron Station
   Alexandria, Virginia 22304-6145

2. Library, Code 52   2
   Naval Postgraduate School
   Monterey, California 93943-5002

3. Chairman, Code EC   1
   Department of Electrical and Computer Engineering
   Naval Postgraduate School
   Monterey, California 93943

4. Professor Fotis A. Papoulias, Code ME/Pa   3
   Department of Mechanical Engineering
   Naval Postgraduate School
   Monterey, California 93943

5. Professor Roberto Cristi, Code EC/Cx   1
   Department of Electrical and Computer Engineering
   Naval Postgraduate School
   Monterey, California 93943

6. Hellenic Army General Staff   1
   Technical Directorate
   Stratopedon Papagou, Cholargos
   Athens, Greece

7. Embassy of Greece   1
   Defense and Army Attache
   2228 Massachusetts Ave., N.W.
   Washington, D.C. 20008

8. Ilías Dimopoulos   1
   Tilephanous 8, Kolonos
   Athens, Greece